DOI 10.5162/iCCC2026/2.4

Implantable MEMS Sensor Platform for Measuring Heart Activity

Sören Schäfer[1*], Peter Detemple[1], Max Haberbusch[2], Oliver Haverbeck[1], Juri Magomajew[1], Francesco Moscato[2], Stefan Schmitt[1]
[1]: Fraunhofer Institute for Microengineering and Microsystems IMM, Mainz, Germany
[2]: Center for Medical Physics and Biomedical Engineering, Medical University of Vienna, Vienna, Austria
[*]soeren.schaefer@imm.fraunhofer.de

Abstract

Heart transplants usually require the severing of the vagus nerve, which connects the heart muscle to the central nervous system. Consequently, the parasympathetic control of the heart, which is responsible for lowering heart activity during periods of relaxation, is impaired. In addition to limitations in the everyday lives of patients, this causes, for example, a permanently elevated resting heart rate and thus accelerated aging of the tissue. One possible solution for restoring the vagal control is to externally stimulate the severed nerve pathway via an implantable electrode array. The response of the heart muscle to a specific stimulation signal must then be detected and ideally be fed back to the stimulation unit.
We report on an implantable sensor platform that is developed for continuous detection of the heart activity. Implanted devices are an attractive alternative to non-invasive measurement methods in terms of reliability and comfort. The MEMS platform has three axially arranged piezoresistive force sensors on a glass substrate, which are encapsulated with a biocompatible material. Ex-vivo tests in a pressure chamber are followed by in-vivo tests on pig hearts, in which cardiac activity is controlled by administering dobutamine. In-vivo stability tests show a reliable measurement signal even after one month and underline the biocompatibility.

1 Introduction

A heart transplant (approximately 3,500 per year worldwide) is the only medical treatment option for patients with end-stage heart failure [1, 2]. However, the denervation of the heart caused by the operation means that the controlled increase and decrease in heart rate can no longer be fully guaranteed (chronotropic incompetence). For patients, this results in limitations in physical endurance and typically an increased resting heart rate. The latter in particular leads to accelerated aging or hardening of the heart muscle tissue (fibrosis) due to permanently increased contraction forces, which usually necessitates another transplant after a few years.

One solution could be targeted stimulation of the vagus nerve connection, e.g., via an implantable electrode interface [3]. The vagus nerve is a central component of the parasympathetic nervous system, which is responsible for rest and relaxation, including the regulation of heart rate. In order to close the feedback loop, in addition to stimulating the nerve, the heart activity must be measured, processed, and evaluated as a response and then fed back to the interface in the next step.

The article describes the development of an implantable MEMS sensor platform that continuously detects cardiac activity using pressure sensors. The challenge here lies in the biocompatible encapsulation of commercial MEMS pressure sensors and the robust electrical signal readout, so that cardiac activity can be measured over the long term without impairing the function of the heart itself. The article is divided into the design of the platform and subsequent ex-vivo and in-vivo tests in a pig model.

2 Concept development

2.1 Approach

Figure 1a) shows an oblique view of the 3D model of an early concept design of the sensor platform. Three pressure sensors are positioned on a rigid substrate, e.g., a glass plate. The entire arrangement, including electrical connections, is then encapsulated with a biocompatible material, e.g., silicone. Figure 1b) schematically shows how the sensor platform is implanted in the heart muscle and illustrates the forces acting on it. The special geometry, shown here as a hillock structure in the encapsulation, ensures that two of the three pressure sensors (S1 and S3) experience a higher force than S2 (F_1, $F_3 > F_2$). In addition to redundancy and an extended measuring range, this should ideally also provide information about the stiffness of the heart muscle tissue, provided that this has an influence on the difference between the respective signals output of S2 over S1 and S3.

2.2 Sensor design

The starting point for implementation is the question of the required dimensions of the platform (maximum sensitivity vs. minimum invasiveness) and the selection of suitable sensors and materials. To estimate the expected forces, analytical models of the stress on the left ventricle are used [4, 5]. Since the encapsulation material dampens the force acting on the sensors, the arrangement shown in Fig. 1b) is examined in an FEM simulation using suitable assumptions for the elasticity modulus of the materials involved. Overall, a value between 12 and 48 kPa is expected for the normal component of the stress. Commercially available

DOI 10.5162/iCCC2026/2.4

piezoresistive elements (SM5108E, Silicon Microstructures, Inc.) were used as bare dies for the sensors. These measure the absolute pressure with a sensitivity of 0.6 mV/kPa and come with a measuring range from 0 to approx. 200 kPa.

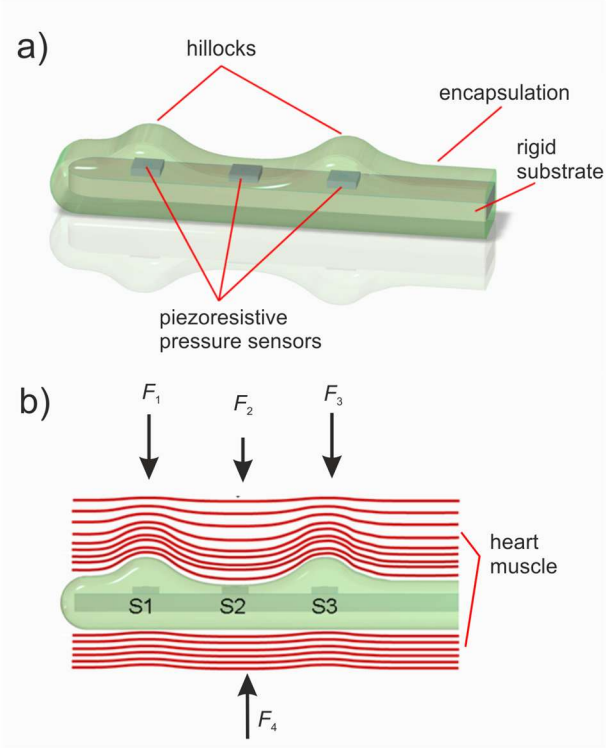

Figure 1 a) 3D model of the sensor concept with three piezoresistive pressure sensors, b) different forces F_1 through F_4 on the sensor platform implanted in the heart muscle.

3 Implementation

Figure 2 shows a 3D model as well as photographs of an unencapsulated sensor platform. A glass plate with dimensions of (27 × 2) mm^2 with lithographically structured Au layers serves as rigid substrate. The deposition of Au layers is in principle a two-step process, starting with a lift-off structuring process for an e-beam evaporated 200 nm-thick layer of Au with Cr/Ni adhesion layers. This serves as a starting layer for an electroplating step during which the Au layer gets thickened up to 3 µm. Afterwards the sensor elements are fixated via epoxy adhesive and wire-bonded to the respective base pads on the substrate. The two outer sensor elements S1 and S3 are positioned on pillars of silicon with the same base area as the sensor element and a height of, here, 3 mm.

The encapsulation process must on the one hand ensure a reliable sealing of the electronics and on the other hand must leave the delicate wire bond contacts intact. It is furthermore important to have a defined thickness of the encapsulation material above the pressure sensors to ensure reproducible results.

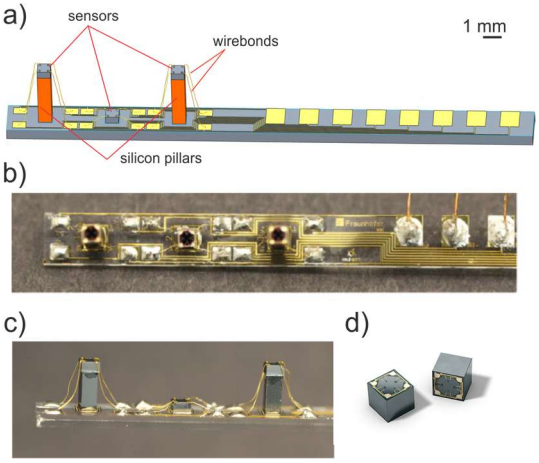

Figure 2 a) 3D model of the unencapsulated sensor platform with sensor elements on pillars of silicon. b), c) electrically connected unencapsulated sensor platform on a glass substrate from top and front view, respectively. d) Image of bare die pressure sensors with dimensions of (0.69 × 0.69 × 0.40) mm^3.

This has been realized by a 3D-printed casting mold that has been modeled based on the topography of the sensor elements as shown in Figs. 3a), b). Once the sensor plate is placed within the mold parts, liquid silicone (Dragonskin) is filled in via the tiny hole in part 3 and left for curing. Figure 3c) shows photographs of the encapsulated front side after demounting from the mold.

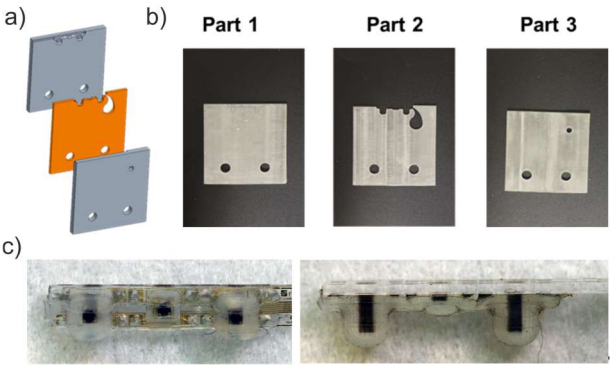

Figure 3 a) 3D model of the three part casting mold. b) Finished 3D-printed mold parts. Silicone is filled in via the tiny hole in part 3. c) top and side views of the encapsulated sensor platform.

DOI 10.5162/iCCC2026/2.4

4 Functional tests

4.1 Ex-vivo

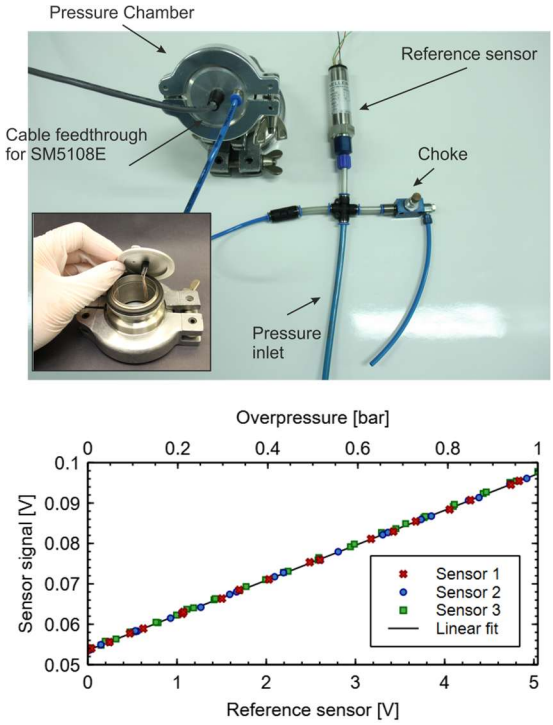

Figure 4 Top shows a photograph of the air-tight pressure chamber containing the connected sensor platform as indicated in the inset. A reference pressure sensor is connected in parallel. Bottom shows the pressure signal of each of the three sensors over the voltage of the reference as well as a linear fit (black line). The markers for each line are reduced for visibility.

First, each encapsulated sensor platform is placed in an in-house built pressure chamber and is tested as shown in Fig. 4. The chamber comes with a cable feedthrough to extract the signal of each of the three sensors. A reference sensor (Omega Keller, type 21S/80549.3) is connected in parallel. The reference sensor and the SM5108E of the platform show 0 V and 53 mV for atmospheric pressure and 5 V and 97 mV for 1 bar overpressure, respectively. All sensors show a linear behavior versus the overpressure. The linear fit yields a slope of 8.6 mV/V which corresponds to a sensitivity of about 0.43 mV/kPa. This is slightly less than the theoretical sensitivity given by the manufacturer but plausible, given that the sensors are encapsulated by a layer of silicone.

In addition, the sensor platform was tested by pressing it into a soft tissue like a block of gelatin or pieces of pork loin (not shown here). The main insight from these tests is that the height differences of S1 and S3 over S2 as shown in Figs. 2 and 3 is too large for S2 to give out a signal. Hence, the height discrepancy was reduced to 200 µm by mounting S2 on a Si pillar as well.

4.2 In-vivo.

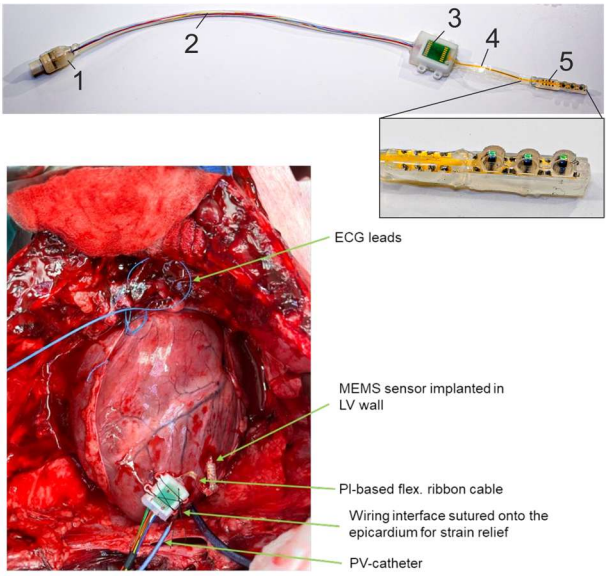

Figure 5 Top photograph shows the device prepared for in-vivo testing: connector (1), wires guided through silicone tubing (2), ASIC for AD conversion (3), custom-made flexible conductor ribbon (4), encapsulated sensor platform (5). Bottom photograph shows the device implanted in the left ventricular wall of a pig heart (courtesy Medical University of Vienna).

After ex-vivo testing, the sensor device is further prepared for in-vivo testing in a pig heart as shown in Fig. 5. The glass substrate is further encapsulated in a thin layer of silicone for protection. The connection to the ADC ASIC [6] is over a custom-made, PI-based flexible ribbon cable for strain relief. Figure 5 additionally shows the in-vivo application in a pigs heart. Here, the sensor array is placed in the left ventricular wall. However, also other positions of the sensors were tested with respect to responsivity.

Figure 6 exemplarily shows the sensor signals as well as electrocardiogram signal (ECG) for two different stages: a) refers to pre and b) to post injection of dobutamine, which stimulates heart activity. The signal level is reduced compared to calibration obtained during calibration in Fig. 4 which is likely due to further encapsulation and ohmic losses. However, the sensors clearly respond to the forces during the cardiac cycle and reflect the heart activity. The instantaneous heart rate can be easily extracted. Other than that, the signal form changes upon administration of dobutamine and indicates a change in contractility. The long term stability and biocompatibility have been evaluated and are described in detail in Ref. [7]. After a 30-day period the signal amplitude of the sensors decreases. However, heart rate and certain signatures of the signal form can still be extracted. Even after 120 days of implantation, no severe immune response has been detected which underlines the biocompatibility.

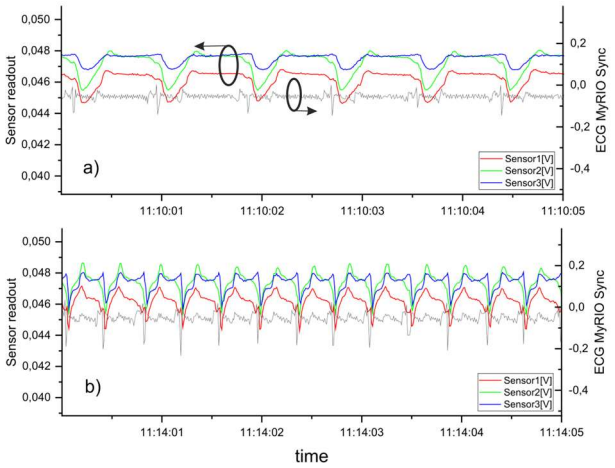

Figure 6 Readout signals of the three sensors in mV during in-vivo testing in a pigs heart. The grey curves indicate the ECG signal. a) and b) refer to before and after injection of dobutamine, respectively.

5 Acknowledgments

We acknowledge the European Commission for funding the H2020-FETPROACT-2018-2020 NEUHEART Project No. 824071, which made this work possible. The authors furthermore thank the collaborators from Sant'Anna University in Pisa, Medizinische Universität Wien and University College London that helped acquiring parts of the shown results. Sören Schäfer. acknowledges funding by the German Federal Ministry of Education and Research in the context of the federal-state program "FH-Personal" under the grant number 03FHP147A (REQUAS).

6 References

[1] E. Y. Birati and J. E. Rame, "Post-heart transplant complications", *Critical care clinics*, vol. 30, no. 3, pp. 629–637, 2014, doi: 10.1016/j.ccc.2014.03.005.

[2] A. Jaiswal *et al.,* "Clinical outcomes of older adults listed for heart transplantation in the United States", *Journal of the American Geriatrics Society*, vol. 69, no. 9, pp. 2507–2517, 2021, doi: 10.1111/jgs.17271.

[3] M. Capogrosso *et al.,* "A brain–spine interface alleviating gait deficits after spinal cord injury in primates" (in En;en), *Nature*, vol. 539, no. 7628, pp. 284–288, 2016, doi: 10.1038/nature20118.

[4] P. Gould, D. Ghista, L. Brombolich, and I. Mirsky, "In vivo stresses in the human left ventricular wall: analysis accounting for the irregular 3-dimensional geometry and comparison with idealised geometry analyses", *Journal of Biomechanics*, vol. 5, no. 5, pp. 521–539, 1972, doi: 10.1016/0021-9290(72)90009-7.

[5] D. N. Ghista and H. Sandler, "An analytic elastic-viscoelastic model for the shape and the forces in the left ventricle", *Journal of Biomechanics*, vol. 2, no. 1, pp. 35–47, 1969, doi: 10.1016/0021-9290(69)90040-2.

[6] N. Neshatvar, M. Schormans, D. Jiang, S. Schmitt, P. Detemple, and A. Demosthenous, "An Implantable Phase Locked Loop MEMS-Based Readout System for Heart Transplantation", *IEEE Trans. Circuits Syst. II*, vol. 69, no. 10, pp. 4168–4172, 2022, doi: 10.1109/TCSII.2022.3190796.

[7] C. Zinno *et al.,* "Implementation of an epicardial implantable MEMS sensor for continuous and real-time postoperative assessment of left ventricular activity in adult minipigs over a short- and long-term period", *APL bioengineering*, vol. 8, no. 2, p. 26102, 2024, doi: 10.1063/5.0169207.